First measurements of the branching fractions of J/ψ and $\psi(3686) \to \Sigma^0\bar{\Sigma}^0\eta$

M. Ablikim *et al.*[*]
(BESIII Collaboration)

(Received 18 August 2026; accepted 26 October 2026; published 16 November 2026)

Based on $(10087 \pm 44) \times 10^6$ J/ψ and $(2712 \pm 14) \times 10^6$ $\psi(3686)$ events collected with the BESIII detector at the BEPCII collider, the hadronic decays $J/\psi \to \Sigma^0\bar{\Sigma}^0\eta$ and $\psi(3686) \to \Sigma^0\bar{\Sigma}^0\eta$ are observed for the first time. The corresponding branching fractions are measured to be $\mathcal{B}(J/\psi \to \Sigma^0\bar{\Sigma}^0\eta) = (7.5 \pm 0.3 \pm 0.8) \times 10^{-5}$ and $\mathcal{B}(\psi(3686) \to \Sigma^0\bar{\Sigma}^0\eta) = (1.3 \pm 0.1 \pm 0.1) \times 10^{-5}$, respectively, where the first uncertainties are statistical, and the second systematic. The ratio $Q \approx \frac{\mathcal{B}(\psi(3686)\to\Sigma^0\bar{\Sigma}^0\eta)}{\mathcal{B}(J/\psi\to\Sigma^0\bar{\Sigma}^0\eta)}$ is determined to be $(17.3 \pm 1.5 \pm 1.7)\%$, which is consistent with the 12%-rule within 3.0σ. No significant intermediate states or threshold enhancements are observed in the Σ^0 ($\bar{\Sigma}^0$) η and $\Sigma^0\bar{\Sigma}^0$ invariant mass spectra.

DOI: 10.1103/5kzp-t345

I. INTRODUCTION

Studies of the hadronic decays of the charmonium states J/ψ and $\psi(3686)$ provide good opportunities to test quantum chromodynamics (QCD) in the transition region between perturbative and nonperturbative regimes [1]. Within perturbative QCD, the ratio of the branching fractions for J/ψ and $\psi(3686)$ decaying into the same final state is predicted to follow the so-called "12%-rule" [2–5], expressed as

$$Q_h = \frac{\mathcal{B}(\psi(3686) \to h)}{\mathcal{B}(J/\psi \to h)} \simeq \frac{\mathcal{B}(\psi(3686) \to e^+e^-)}{\mathcal{B}(J/\psi \to e^+e^-)} \simeq 12\%, \tag{1}$$

where h denotes any exclusive hadronic decay mode. Many measured decays are consistent with this prediction within uncertainties. However, this rule was first observed to be violated in the process $\psi(2S) \to \rho\pi$, which is known as the "$\rho\pi$ puzzle" [6,7]. Subsequent experimental studies have revealed further deviations from the 12% ratio, such as in the isospin-violating decay J/ψ and $\psi(3686) \to \Lambda\bar{\Lambda}\pi^0$, in contrast to the isospin-conserving decay J/ψ and $\psi(3686) \to \Lambda\bar{\Lambda}\eta$ [8]. Further measurements of baryonic final states are essential for improving our understanding of the origin of these discrepancies.

Many fundamental issues in baryon spectroscopy remain poorly understood. Charmonium decays offer an excellent platform for studying excited nucleons and hyperons—N^*, Λ^*, Σ^*, and Ξ^* [9]. Specifically, three-body decays like $B\bar{B}P$, where B denotes a baryon and P represents a pseudoscalar meson (π, η), provide a powerful avenue to search for excited baryon states. Enhancements near the baryon-antibaryon threshold have been observed in charmonium and B meson decays [10,11]. Numerous theoretical proposals, including gluonic mechanisms, fragmentation mechanisms, baryonia, multiquark states, and final-state interactions, have been proposed to explain these structures [12]. More searches for such enhancements across different quantum numbers and production channels are valuable for distinguishing between these models. The BESIII experiment has collected the world's largest J/ψ and $\psi(3686)$ datasets [13,14], thereby providing a unique opportunity to explore those states.

In this work, we report the first observations and branching fraction measurements of $J/\psi \to \Sigma^0\bar{\Sigma}^0\eta$ and $\psi(3686) \to \Sigma^0\bar{\Sigma}^0\eta$ using $(10087 \pm 44) \times 10^6$ J/ψ and $(2712 \pm 14) \times 10^6$ $\psi(3686)$ events collected with the BESIII detector at the BEPCII collider. Based on these measurements, we test the 12%-rule in the $J/\psi \to \Sigma^0\bar{\Sigma}^0\eta$ and $\psi(3686) \to \Sigma^0\bar{\Sigma}^0\eta$ decays. Potential intermediate states or threshold enhancements in the $\Sigma^0\bar{\Sigma}^0\eta$ and $\Sigma^0\bar{\Sigma}^0$ mass spectra are also examined.

II. BESIII DETECTOR AND MONTE CARLO SIMULATION

The BESIII detector [15] records symmetric e^+e^- collisions provided by the BEPCII storage ring [16] in the center-of-mass energy range from 1.84 to 4.95 GeV, with a peak luminosity of 1.1×10^{33} cm^{-2} s^{-1} achieved at $\sqrt{s} = 3.773$ GeV. BESIII has collected large data samples in this energy region [17–19]. The cylindrical core of the

[*]Full author list given at the end of the article.

Published by the American Physical Society under the terms of the Creative Commons Attribution 4.0 International license. Further distribution of this work must maintain attribution to the author(s) and the published article's title, journal citation, and DOI. Funded by SCOAP[3].

BESIII detector covers 93% of the full solid angle and consists of a helium-based multilayer drift chamber (MDC), a time-of-flight system (TOF), and a CsI(Tl) electromagnetic calorimeter (EMC), which are all enclosed in a superconducting solenoidal magnet providing a 1.0 T magnetic field. The magnetic field was 0.9 T in 2012. The solenoid is supported by an octagonal flux-return yoke with resistive plate counter muon identification modules interleaved with steel. The charged-particle momentum resolution at 1 GeV/c is 0.5%, and the dE/dx resolution is 6% for electrons from Bhabha scattering. The EMC measures photon energies with a resolution of 2.5% (5%) at 1 GeV in the barrel (end cap) region. The time resolution in the plastic scintillator TOF barrel region is 68 ps, while that in the end cap region was 110 ps. The end cap TOF system was upgraded in 2015 using multigap resistive plate chamber technology, achieving a time resolution of 60 ps. This upgrade benefits 87% of the J/ψ data sample and 83% of the $\psi(3686)$ data sample used in this analysis, enhancing particle identification for these datasets [20–22].

This analysis is performed using BESIII Offline Software System [23]. To investigate potential background and optimize event selection criteria, samples of inclusive J/ψ and $\psi(3686)$ Monte Carlo (MC) events are produced. The production of the J/ψ or $\psi(3686)$ resonance is simulated by the MC event generator KKMC [24] including the beam energy spread, and the decays are generated by EVTGEN [25,26] for known decay modes with branching fractions being set to the Particle Data Group (PDG) world average values [27], and by LUNDCHARM [28] for the remaining unknown decays. To evaluate the detection efficiencies and optimize the event selection criteria, samples of 0.2 million phase space (PHSP) MC events [29] are generated for each data-taking year, taking into account the corresponding detector conditions.

III. EVENT SELECTION

In the channel $\psi(3686) \to \Sigma^0\bar{\Sigma}^0\eta$, the Σ^0 and $\bar{\Sigma}^0$ baryons are reconstructed via the $\gamma\Lambda$ and $\gamma\bar{\Lambda}$ decays, respectively. The η meson is reconstructed via the $\eta \to \gamma\gamma$ decay mode, while the Λ and $\bar{\Lambda}$ are reconstructed via the $p\pi^-$ and $\bar{p}\pi^+$ modes, respectively.

Charged tracks detected in the MDC are required to be within a polar angle (θ) range of $|\cos\theta| < 0.93$, where θ is defined with respect to the detector symmetry axis (z-axis), and their distance of closest approach to the interaction point must be less than 20 cm along the z-axis (R_z) and less than 10 cm in the transverse plane (R_{xy}). Particle identification (PID) for charged tracks combines measurements of the energy deposited in the MDC (dE/dx) and the flight time in the TOF to form likelihoods $\mathcal{L}(h)$ ($h = p$, K, π) for each hadron h hypothesis. Each track is assigned as the particle type with the greatest PID likelihood. At least two oppositely charged protons and pions are required in each event. Photon candidates are identified using isolated showers in the EMC. The deposited energy of each shower must be more than 25 MeV in the barrel region ($|\cos\theta| < 0.80$) and more than 50 MeV in the end cap region ($0.86 < |\cos\theta| < 0.92$). To suppress electronic noise and showers unrelated to the event, the difference between the EMC time and the event start time is required to be within [0, 700] ns. After the above track-level requirements, the candidate events with at least four good photons are selected.

The $\Lambda(\bar{\Lambda})$ candidates are reconstructed by combining identified (anti)protons with oppositely charged pion tracks and performing a secondary vertex fit. The candidate with the minimum $\chi^2_\Lambda(\chi^2_{\bar{\Lambda}})$ value is selected. After reconstructing the Λ and $\bar{\Lambda}$ candidates, no additional charged track within $R_{xy} < 1.0$ cm and $R_z < 10.0$ cm remains.

To improve momentum resolution and suppress background, a four-constraint (4C) kinematic fit enforcing energy-momentum conservation is performed under the hypothesis of $\Lambda\bar{\Lambda}\gamma\gamma\gamma\gamma$. The fit constrains the total four-momentum of the final-state particles to that of the initial e^+e^- system. For events with more than four photons, the $\Lambda\bar{\Lambda}\gamma\gamma\gamma\gamma$ combination with the minimum $\chi^2_{\rm 4C}$ is retained. Additionally, a requirement of $\chi^2_{\rm 4C} < 60$ is imposed for $J/\psi \to \Sigma^0\bar{\Sigma}^0\eta$, while $\chi^2_{\rm 4C} < 40$ is required for $\psi(3686) \to \Sigma^0\bar{\Sigma}^0\eta$. The $\chi^2_{\rm 4C}$ requirements are optimized to maximize the figure of merit defined as $S/\sqrt{S+B}$, where S is the signal yield and B is the background yield from the inclusive MC sample. The Σ^0, $\bar{\Sigma}^0$ and η candidates are selected by minimizing $\chi^2_{\Sigma^0\bar{\Sigma}^0\eta} \equiv \frac{(M_{\gamma_1\gamma_2}-M_\eta)^2}{\sigma^2_\eta} + \frac{(M_{\gamma_3\Lambda}-M_{\Sigma^0})^2}{\sigma^2_{\Sigma^0}} + \frac{(M_{\gamma_4\bar{\Lambda}}-M_{\bar{\Sigma}^0})^2}{\sigma^2_{\bar{\Sigma}^0}}$, where M_η, M_{Σ^0} and $M_{\bar{\Sigma}^0}$ are the masses of η and Σ cited from the PDG [27], respectively, σ_η and σ_Σ are the mass resolutions of η and Σ determined from signal MC samples. The Σ^0, $\bar{\Sigma}^0$ and η candidates are required to satisfy $|M_{\gamma\Lambda} - m_{\Sigma^0}| < 15$ MeV/c^2, $|M_{\gamma\bar{\Lambda}} - m_{\bar{\Sigma}^0}| < 15$ MeV/c^2 and $|M_{\gamma\gamma} - m_\eta| < 25$ MeV/c^2, respectively.

To suppress background events containing π^0 mesons, the π^0 candidates are selected by minimizing $|M_{\gamma\gamma} - M_{\pi^0}|$, where M_{π^0} is the nominal π^0 mass from the PDG [27]. A requirement of $|M_{\gamma\gamma} - M_{\pi^0}| > 20$ MeV/c^2 is applied, corresponding to approximately three times the mass resolution. For the process $\psi(3686) \to \Sigma^0\bar{\Sigma}^0\eta$, to reject backgrounds originating from $\psi(3686) \to \eta J/\psi$ with the subsequent decay $J/\psi \to \Sigma^0\bar{\Sigma}^0$, the requirement $|M_{\Sigma^0\bar{\Sigma}^0} - M_{J/\psi}| > 30$ MeV/c^2 is imposed, where $M_{J/\psi}$ denotes the nominal J/ψ mass taken from the PDG [27]. For $J/\psi \to \Sigma^0\bar{\Sigma}^0\eta$, to suppress the backgrounds with one fewer photon, an additional 4C kinematic fit under the hypothesis of $J/\psi \to \Lambda\bar{\Lambda}\gamma\gamma\gamma$ is performed for all possible photon combinations. The combination with the minimum $\chi^2_{\gamma\gamma\gamma}$ is selected and compared with the $\chi^2_{4\,\rm c}$ from the signal hypothesis. Events with $\chi^2_{\gamma\gamma\gamma} < \chi^2_{\rm 4C}$ are discarded.

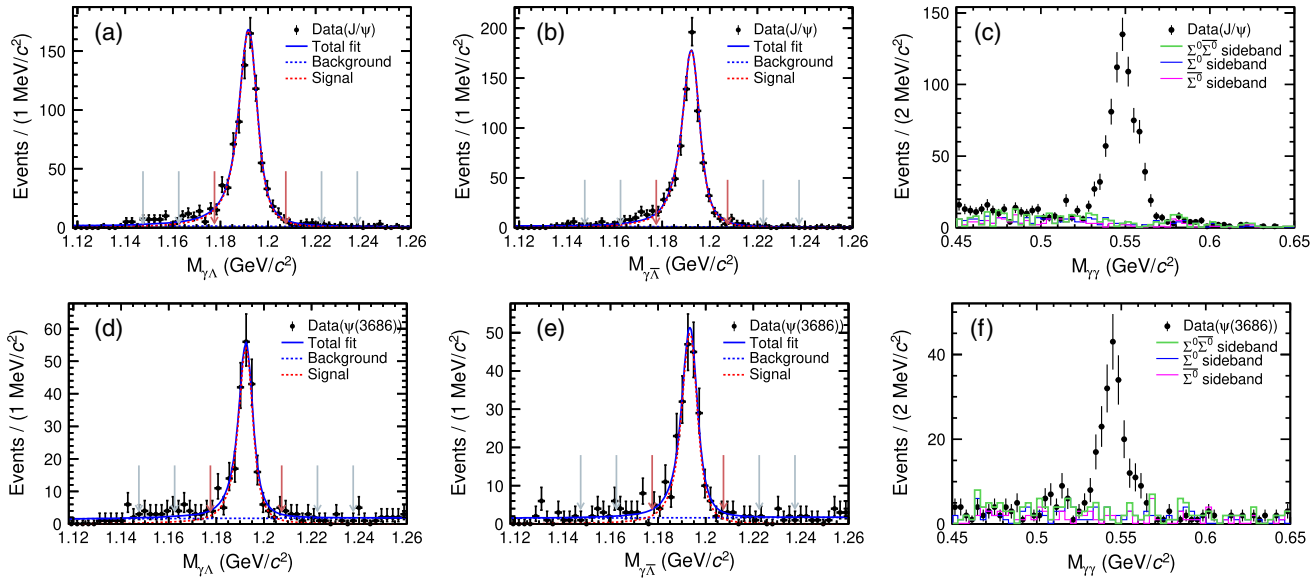


FIG. 1. Invariant mass distributions of $\gamma\Lambda$ (a,d), $\gamma\bar{\Lambda}$ (b,e), $\gamma\gamma$ (c,f) for $J/\psi \to \Sigma^0\bar{\Sigma}^0\eta$ (top) and $\psi(3686) \to \Sigma^0\bar{\Sigma}^0\eta$ (bottom). The dots with error bars are the data, the blue solid lines give the total fit results, the red dashed lines are the signal components, and the blue dashed lines are the smooth backgrounds. The red and gray solid arrows show the Σ^0 or $\bar{\Sigma}^0$ signal and sideband regions, respectively.

Potential backgrounds are studied using the inclusive MC samples, which include 10 billion J/ψ events and 2.7 billion $\psi(3686)$ events. No significant peaking background is observed in the invariant mass distribution of the $\gamma\gamma$. Therefore, the two-dimensional $\Sigma^0\bar{\Sigma}^0$ sideband method is used to estimate combinatorial backgrounds by combining background events in the Σ^0 and $\bar{\Sigma}^0$ sideband regions: $[1.1475, 1.1625]$ GeV/c^2 and $[1.2225, 1.2375]$ GeV/c^2. The scale factor is determined by fitting the Σ^0 and $\bar{\Sigma}^0$ mass spectra, where the signal shape is described by the signal MC shape convolved with a Gaussian resolution function, while the background shape is described by a linear function. The fit results are shown in Fig. 1. The distributions of $M_{\gamma\gamma}$ from the $\Sigma^0 - \bar{\Sigma}^0$ two-dimensional sideband region are shown in Fig. 1(c) and (f).

To estimate the background yield from continuum light hadron production, which originates directly from e^+e^- annihilation rather than $\psi(3686)$ decays, we perform the same analysis procedure on the data samples at center-of-mass energies of 3.65 GeV, 3.682 GeV, and 3.773 GeV. No event remains after applying all the selection requirements for the data taken at 3.65 and 3.682 GeV, and only one event remains at 3.773 GeV. Due to limited statistics and the absence of structures significantly different from statistical fluctuations, the background from continuum light hadron production is neglected.

IV. BRANCHING-FRACTION DETERMINATION

To extract the signal yield, an unbinned maximum-likelihood fit is performed on the $M_{\gamma\gamma}$ distribution, where the signal is described by the MC-simulated shape

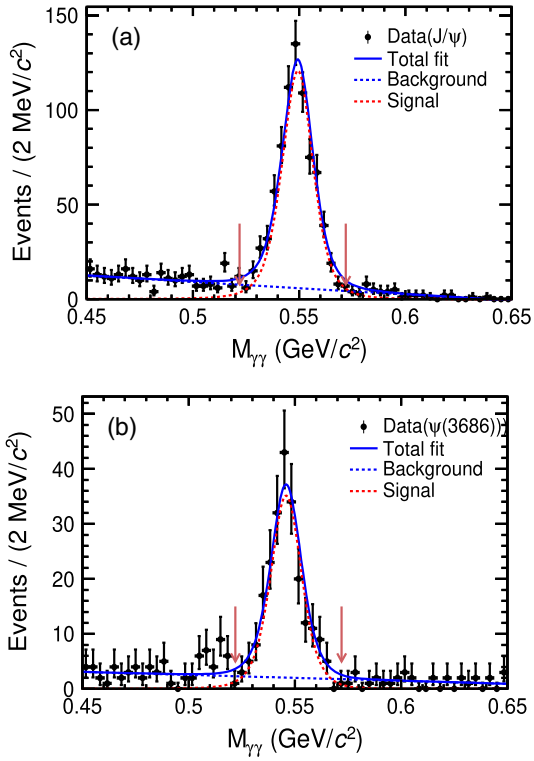


FIG. 2. Fits to the $M_{\gamma\gamma}$ distributions for the data. The top and bottom figures are the (a) J/ψ and (b) $\psi(3686)$ samples, respectively. The dots with error bars show the data, the blue solid lines give the total fit results, the red dashed lines are the signal components, and the blue dashed lines are the smooth backgrounds. The region marked by the red arrows denotes the signal region.

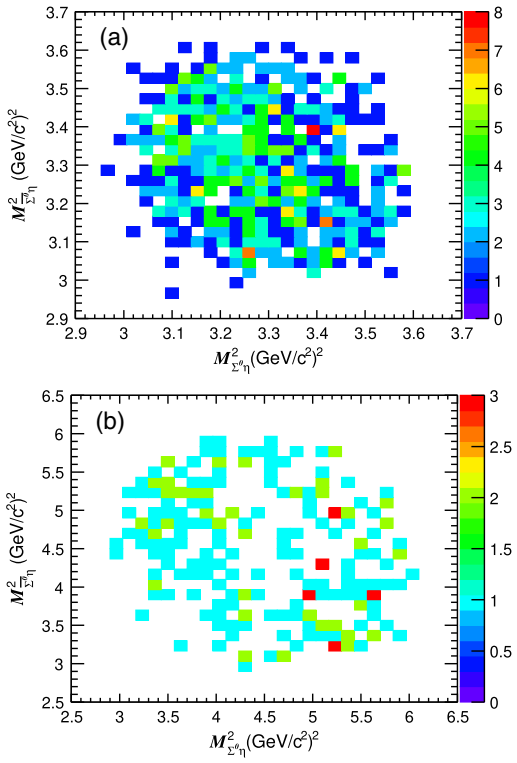


FIG. 3. The Dalitz plots of $M^2(\Sigma^0\eta)$ versus $M^2(\bar{\Sigma}^0\eta)$ from the data samples of (a) J/ψ and (b) $\psi(3686)$.

convolved with a Gaussian function with free parameters in the fit to account for the resolution difference between data and MC simulation, and the background is described by a linear function. Figure 2 shows the fitting results of $M_{\gamma\gamma}$, from which the signal yields are determined to be 193 ± 15 and 732 ± 30 for $\psi(3686) \to \Sigma^0\bar{\Sigma}^0\eta$ and $J/\psi \to \Sigma^0\bar{\Sigma}^0\eta$, respectively.

The Dalitz plot of $M^2(\Sigma^0\eta)$ versus $M^2(\bar{\Sigma}^0\eta)$ from the background-subtracted data sample is presented in Fig. 3. Given the significant discrepancy between the data and the PHSP MC simulation (shown in Fig. 4), the PHSP MC sample cannot provide an accurate estimate of the signal detection efficiency. To reliably determine the detection efficiencies, an event-by-event weighting method is applied, in which PHSP MC events are reweighted according to the observed mass distribution. Specifically, the weight factor is derived from the two-dimensional ratio between the data and the PHSP MC in the $\Sigma^0\eta$ versus $\overline{\Sigma^0}\eta$ Dalitz plot, and is used to correct the signal MC sample. The specific formula is used to determine the signal detection efficiency(ε_w) as follows:

$$\varepsilon_w \equiv \frac{\sum_{i=1}^{N^{\text{selected}}} w_i}{\sum_{i=1}^{N^{\text{generated}}} w_i}. \tag{2}$$

Here, ω_i represents the weight factor for the event i of the PHSP MC sample, while N^{selected} and $N^{\text{generated}}$ denote the numbers of selected and generated events, respectively. The final efficiencies are 0.6% and 3.4% for the J/ψ and $\psi(3686)$ decays, respectively.

The branching fraction of the $\psi(3686) \to \Sigma^0\bar{\Sigma}^0\eta$ decay is calculated by

$$\mathcal{B}(\psi' \to \Sigma^0\bar{\Sigma}^0\eta) \equiv \frac{N_{\text{sig}}}{N_{\psi'} \cdot \varepsilon_w \cdot \mathcal{B}_1^2 \cdot \mathcal{B}_2^2 \cdot \mathcal{B}_3}, \tag{3}$$

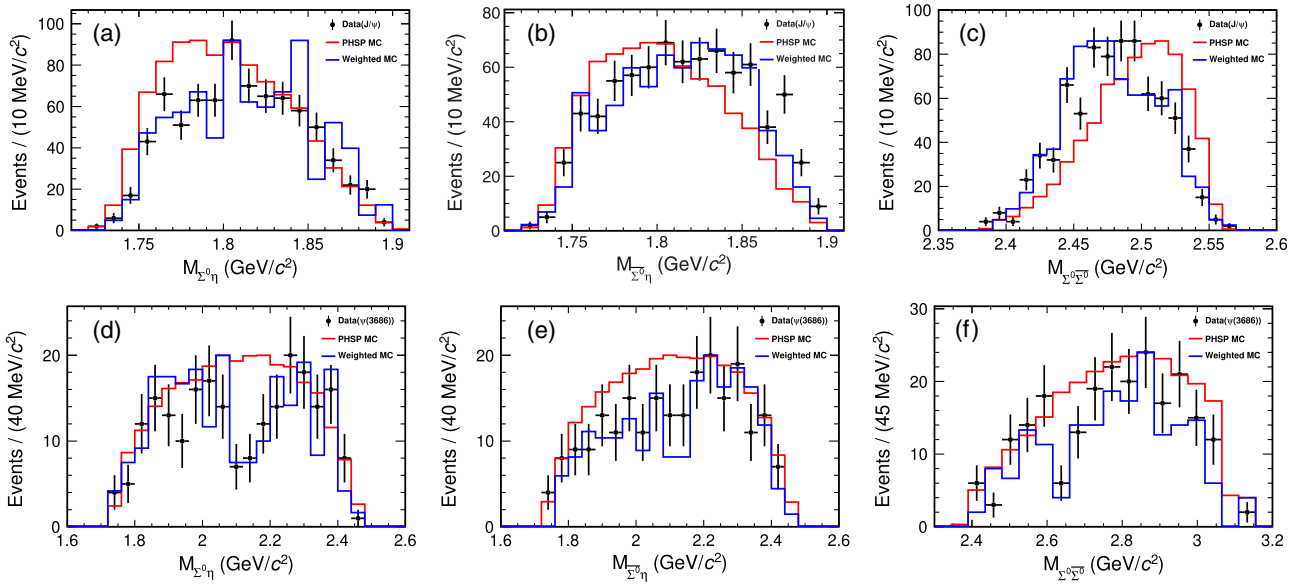


FIG. 4. Invariant mass distributions of $\Sigma^0\eta$ (a,d), $\bar{\Sigma}^0\eta$ (b,e) and $\Sigma^0\bar{\Sigma}^0$ (c,f) for J/ψ (top) and $\psi(3686)$ (bottom). The black dots with error bars represent data, the red solid histograms represent the PHSP MC simulations, and the blue solid histograms represent the reweighted MC simulation.

where $N_{\psi'}$ is the total number of $\psi(3686)$ [13] or J/ψ [14] events in the data; and $\mathcal{B}_1$, $\mathcal{B}_2$, and $\mathcal{B}_3$ are the branching fractions of $\Sigma^0 \to \gamma\Lambda$, $\Lambda \to p\pi^-$ and $\eta \to \gamma\gamma$ quoted from the PDG [27], respectively. Finally, we obtain $\mathcal{B}(\psi(3686) \to \Sigma^0\bar{\Sigma}^0\eta) = (1.3 \pm 0.1) \times 10^{-5}$ and $\mathcal{B}(J/\psi \to \Sigma^0\bar{\Sigma}^0\eta) = (7.5 \pm 0.3) \times 10^{-5}$, where the uncertainties are statistical only.

No evidence is observed for excited Σ^* states or threshold enhancements in the Σ^0 ($\bar{\Sigma}^0$) η and $\Sigma^0\bar{\Sigma}^0$ invariant mass spectra.

V. SYSTEMATIC UNCERTAINTY

The sources of systematic uncertainties are summarized as follows. The uncertainties in the measurements of the total numbers of J/ψ and $\psi(3686)$ events in data are 0.4% [14] and 0.5% [13], respectively, and the uncertainty of the photon detection is 0.5% [30] per photon. The systematic uncertainty due to the $\Lambda/\bar{\Lambda}$ reconstruction is estimated to be 2% [31].

To estimate the systematic uncertainty arising from the 4C kinematic fit, corrections to the helix parameters of the MC simulation are applied to better align the MC with the data [8]. The difference in signal efficiencies between the corrected and uncorrected cases is 0.1% for $J/\psi \to \Sigma^0\bar{\Sigma}^0\eta$ and is neglected for $\psi(3686) \to \Sigma^0\bar{\Sigma}^0\eta$.

The branching fractions of the subresonances are quoted from the PDG [27], with their uncertainties of 0.8%, 0.8% and 0.5% for $\mathcal{B}(\Lambda \to p\pi^-)$, $\mathcal{B}(\bar{\Lambda} \to \bar{p}\pi^+)$ and $\mathcal{B}(\eta \to \gamma\gamma)$, respectively. The total uncertainty from the quoted branching fractions is 1.7% obtained by adding the individual contributions in quadrature.

To estimate the uncertainty of the MC model, the 3-body MC generator is used, with efficiency-corrected Dalitz plots of the $M^2_{\Sigma^0\eta}$ and $M^2_{\bar{\Sigma}^0\eta}$ distributions as inputs. Background events in data are subtracted using the two-dimensional sideband method. To investigate the systematic uncertainties introduced by efficiency calculations using the two-dimensional weighting method, a new background-subtracted MC sample is generated, where the number of background events is fixed to the value determined by the background events counted in the $\Sigma^0\bar{\Sigma}^0$ two-dimensional mass from the final fit results. Then, the input Dalitz plot is updated to the new background-subtracted data when simulating the signal decay process. The changes in efficiencies are assigned as the systematic uncertainties, which are 7.1% for $J/\psi \to \Sigma^0\bar{\Sigma}^0\eta$ and 0.3% for $\psi(3686) \to \Sigma^0\bar{\Sigma}^0\eta$.

The systematic uncertainties from the mass resolution are estimated by fitting the mass spectrum with the MC shape convolved with a fixed-parameter Gaussian function, where the fixed parameters are extracted from the control sample of $J/\psi \to \Sigma^0\bar{\Sigma}^0$. The changes in detection efficiencies, 2.3% for $J/\psi \to \Sigma^0\bar{\Sigma}^0\eta$ and 1.4% for $\psi(3686) \to \Sigma^0\bar{\Sigma}^0\eta$, are assigned as the corresponding systematic uncertainties.

TABLE I. Relative systematic uncertainties in the branching fraction measurements.

Source	J/ψ(%)	$\psi(3686)$(%)
$N_{\psi'}$	0.4	0.5
Photon detection[a]	2.0	2.0
$\Lambda\bar{\Lambda}$ reconstruction[a]	2.8	2.8
Kinematic fit[a]	0.1	0.0
Quoted branching fractions[a]	1.7	1.7
MC model	7.1	0.3
Mass window[a]	2.3	1.4
Fit procedure	5.5	2.6
Total	10.0	4.9

[a]Where the items marked with are common for both decays.

The systematic uncertainties from the fitting procedure include the fit range, the signal shape, and the background shape. To estimate the systematic uncertainties from the fit range, several alternative fits are performed over different intervals: ($[0.44, 0.64]$ GeV/c^2, $[0.46, 0.66]$ GeV/c^2, $[0.44, 0.66]$ GeV/c^2, $[0.46, 0.64]$ GeV/c^2). The largest resulting difference in signal yield is taken as the corresponding systematic uncertainty. To estimate the uncertainty due to the signal shape, the signal MC shape convolved with a Gaussian function with free parameters is used to fit the η and Σ mass distributions in the data. The difference in efficiencies before and after smearing the Gaussian resolution function is taken as the systematic uncertainty. To estimate the uncertainties from the smooth background shape, the fitting function is changed from a first-order Chebyshev polynomial to a third-order one. The difference in the fitted signal yields between the nominal and the alternative background shapes is taken as the corresponding systematic uncertainty. The systematic uncertainties of the fitting procedure are 5.5% for $J/\psi \to \Sigma^0\bar{\Sigma}^0\eta$ and 2.6% for $\psi(3686) \to \Sigma^0\bar{\Sigma}^0\eta$.

The total systematic uncertainties are found to be 10.0% for J/ψ and 4.9% for $\psi(3686)$, after adding all contributions in quadrature. All systematic uncertainties are listed in Table I.

VI. SUMMARY

Using $(10087 \pm 44) \times 10^6$ J/ψ and $(2712 \pm 14) \times 10^6$ $\psi(3686)$ events collected with the BESIII detector, the decays $J/\psi \to \Sigma^0\bar{\Sigma}^0\eta$ and $\psi(3686) \to \Sigma^0\bar{\Sigma}^0\eta$ are observed for the first time, and the corresponding branching fractions are measured to be $\mathcal{B}(J/\psi \to \Sigma^0\bar{\Sigma}^0\eta) = (7.5 \pm 0.3 \pm 0.8) \times 10^{-5}$ and $\mathcal{B}(\psi(3686) \to \Sigma^0\bar{\Sigma}^0\eta) = (1.3 \pm 0.1 \pm 0.1) \times 10^{-5}$, where the first uncertainties are statistical and the second systematic. The Q value is determined to be $(17.3 \pm 1.5 \pm 1.7)$%, which is consistent with the 12%-rule within 3.0σ. Here, the common systematic uncertainties of tracking, PID, photon reconstruction, mass window and cited branching fractions have been

canceled. In addition, no significant structures are observed in the Σ^0 ($\bar{\Sigma}^0$) η and $\Sigma^0\bar{\Sigma}^0$ invariant mass spectra.

ACKNOWLEDGMENTS

The BESIII Collaboration thanks the staff of BEPCII [32] and the IHEP computing center for their strong support. This work is supported in part by National Key R&D Program of China under Contracts No. 2023YFA1609400, No. 2025YFA1613900, No. 2023YFA1606000, No. 2023YFA1606704; National Natural Science Foundation of China (NSFC) under Contracts No. 11635010, No. 11935015, No. 11935016, No. 11935018, No. 12025502, No. 12035009, No. 12035013, No. 12061131003, No. 12192260, No. 12192261, No. 12192262, No. 12192263, No. 12192264, No. 12192265, No. 12221005, No. 12225509, No. 12235017, No. 12342502, No. 12361141819, No. 12535005, No. 12305085; the Natural Science Foundation of Henan Province No. 252300421214; the Chinese Academy of Sciences (CAS) Large-Scale Scientific Facility Program; the Strategic Priority Research Program of Chinese Academy of Sciences under Contract No. XDA0480600; CAS under Contract No. YSBR-101; 100 Talents Program of CAS; The Institute of Nuclear and Particle Physics (INPAC) and Shanghai Key Laboratory for Particle Physics and Cosmology; ERC under Contract No. 758462; German Research Foundation DFG under Contract No. FOR5327; Istituto Nazionale di Fisica Nucleare, Italy; Knut and Alice Wallenberg Foundation under Contracts Nos. 2021.0174, 2021.0299, 2023.0315; Ministry of Development of Turkey under Contract No. DPT2006K-120470; National Research Foundation of Korea under Contract No. NRF-2022R1A2C1092335; National Science and Technology fund of Mongolia; Polish National Science Centre under Contract No. 2024/53/B/ST2/00975; STFC (United Kingdom); Swedish Research Council under Contract No. 2019.04595; U.S. Department of Energy under Contract No. DE-FG02-05ER41374.

DATA AVAILABILITY

There are no publicly available research data or software supporting this manuscript. Requests for further information or data should be sent to the authors.

[1] S. L. Olsen, T. Skwarnicki, and D. Zieminska, Rev. Mod. Phys. **90**, 015003 (2018).
[2] G. Karl and W. Roberts, Phys. Lett. **149B**, 263 (1984).
[3] S. J. Brodsky, G. P. Lepage, and S. F. Tuan, Phys. Rev. Lett. **59**, 621 (1987).
[4] M. Chaichian and N. A. Tornqvist, Nucl. Phys. **B323**, 75 (1989).
[5] S. S. Pinsky, Phys. Lett. B **236**, 479 (1990).
[6] W. S. Hou and A. Soni, Phys. Rev. Lett. **50**, 569 (1983).
[7] M. E. B. Franklin *et al.*, Phys. Rev. Lett. **51**, 963 (1983).
[8] M. Ablikim *et al.* (BESIII Collaboration), Phys. Rev. D **87**, 052007 (2013).
[9] B. S. Zou, Nucl. Phys. **A684**, 330 (2001).
[10] M. Ablikim *et al.* (BESIII Collaboration), Phys. Rev. D **71**, 072006 (2005).
[11] Y. J. Lee *et al.* (BELLE Collaboration), Phys. Rev. Lett. **93**, 211801 (2004).
[12] C. W. Bauer, Z. Ligeti, M. Luke, A. V. Manohar, and M. Trott, Phys. Rev. D **70**. 094017 (2004).
[13] M. Ablikim *et al.* (BESIII Collaboration), Chin. Phys. C **48**, 093001 (2024).
[14] M. Ablikim *et al.* (BESIII Collaboration), Chin. Phys. C **41**, 013001 (2017).
[15] M. Ablikim *et al.* (BESIII Collaboration), Nucl. Instrum. Methods Phys. Res., Sect. A **614**, 345 (2010).
[16] C. H. Yu *et al.*, *Proceedings of IPAC2016, Busan, Korea* (JACoW, Busan, 2016).
[17] M. Ablikim *et al.* (BESIII Collaboration), Chin. Phys. C **44**, 040001 (2020).
[18] J. Lu, Y. J. Xiao, and X. Ji, Radiat. Detect. Technol. Methods **4**, 337 (2020).
[19] Y. Cheng, H. Li, Y. Bi *et al.*, Radiat. Detect. Technol. Methods **6**, 418 (2022).
[20] X. Li *et al.*, Radiat. Detect Tech. Methods **1**, 13 (2017).
[21] Y. X. Guo *et al.*, Radiat. Detect Tech. Methods **1**, 15 (2017).
[22] P. Cao *et al.*, Nucl. Instrum. Methods Phys. Res., Sect. A **953**, 163053 (2020).
[23] W. D. Li *et al.*, in *Proceeding of Computing in High Energy and Nuclear Physics (CHEP'06)* (Mumbai, India, 2006).
[24] S. Jadach and B. F. L. Ward, and Z. Wąs, Comput. Phys. Commun. **130**, 260 (2000).
[25] R. G. Ping, Chin. Phys. C **32**, 599 (2008).
[26] D. J. Lange, Nucl. Instrum. Methods Phys. Res., Sect. A **462**, 152 (2001).
[27] R. L. Workmanetal *et al.* (Particle Data Group), Prog. Theor. Exp. Phys. **2025**, 030001 (2024).
[28] J. C. Chen, G. S. Huang, X. R. Qi, D. H. Zhang, and Y. S. Zhu, Phys. Rev. D **62**, 034003 (2000).
[29] R. E. Sanderson and A. Helmi, Mon. Not. R. Astron. Soc **435**, 378 (2013).
[30] M. Ablikim *et al.* (BESIII Collaboration), J. High Energy Phys. 08 (2024) 180.
[31] M. Ablikim *et al.* (BESIII Collaboration), Phys. Rev. D **95**, 052003 (2017).
[32] https://cstr.cn/31109.02.BEPC.

M. Ablikim,[1] M. N. Achasov,[4,d] P. Adlarson,[83] X. C. Ai,[89] C. S. Akondi,[31a,31b] R. Aliberti,[39] A. Amoroso,[82a,82c] Q. An,[79,65,a] Y. H. An,[89] Y. Bai,[63] O. Bakina,[40] H. R. Bao,[71] X. L. Bao,[50] M. Barbagiovanni,[82c] V. Batozskaya,[1,49] K. Begzsuren,[35] N. Berger,[39] M. Berlowski,[49] M. B. Bertani,[30a] D. Bettoni,[31a] F. Bianchi,[82a,82c] E. Bianco,[82a,82c] A. Bortone,[82a,82c] I. Boyko,[40] R. A. Briere,[5] A. Brueggemann,[76] D. Cabiati,[82a,82c] H. Cai,[84] M. H. Cai,[42,l,m] X. Cai,[1,65] A. Calcaterra,[30a] G. F. Cao,[1,71] N. Cao,[1,71] S. A. Cetin,[69a] X. Y. Chai,[51,i] J. F. Chang,[1,65] T. T. Chang,[48] G. R. Che,[48] Y. Z. Che,[1,65,71] C. H. Chen,[10] Chao Chen,[1] G. Chen,[1] H. S. Chen,[1,71] H. Y. Chen,[20] M. L. Chen,[1,65,71] S. J. Chen,[47] S. M. Chen,[68] T. Chen,[1,71] W. Chen,[50] X. R. Chen,[34,71] X. T. Chen,[1,71] X. Y. Chen,[12,h] Y. B. Chen,[1,65] Y. Q. Chen,[16] Z. K. Chen,[66] J. Cheng,[50] L. N. Cheng,[48] S. K. Choi,[11] X. Chu,[12,h] G. Cibinetto,[31a] F. Cossio,[82c] J. Cottee-Meldrum,[70] H. L. Dai,[1,65] J. P. Dai,[87] X. C. Dai,[68] A. Dbeyssi,[19] R. E. de Boer,[3] D. Dedovich,[40] C. Q. Deng,[80] Z. Y. Deng,[1] A. Denig,[39] I. Denisenko,[40] M. Destefanis,[82a,82c] F. De Mori,[82a,82c] E. Di Fiore,[31a,31b] X. X. Ding,[51,i] Y. Ding,[44] Y. X. Ding,[32] Yi. Ding,[38] J. Dong,[1,65] L. Y. Dong,[1,71] M. Y. Dong,[1,65,71] X. Dong,[84] Z. J. Dong,[66] M. C. Du,[1] S. X. Du,[89] Shaoxu Du,[12,h] X. L. Du,[12,h] Y. Q. Du,[84] Y. Y. Duan,[61] Z. H. Duan,[47] P. Egorov,[40,b] G. F. Fan,[47] J. J. Fan,[20] Y. H. Fan,[50] J. Fang,[1,65] Jin Fang,[66] S. S. Fang,[1,71] W. X. Fang,[1] Y. Q. Fang,[1,65,a] L. Fava,[82b,82c] F. Feldbauer,[3] G. Felici,[30a] C. Q. Feng,[79,65] J. H. Feng,[16] L. Feng,[42,l,m] Q. X. Feng,[42,l,m] Y. T. Feng,[79,65] M. Fritsch,[3] C. D. Fu,[1] J. L. Fu,[71] Y. W. Fu,[1,71] H. Gao,[71] Xu Gao,[38] Y. Gao,[79,65] Y. N. Gao,[51,i] Y. Y. Gao,[32] Yunong Gao,[20] Z. Gao,[48] S. Garbolino,[82c] I. Garzia,[31a,31b] L. Ge,[63] P. T. Ge,[20] Z. W. Ge,[47] C. Geng,[66] E. M. Gersabeck,[75] A. Gilman,[77] K. Goetzen,[13] J. Gollub,[3] J. B. Gong,[1,71] J. D. Gong,[38] L. Gong,[44] W. X. Gong,[1,65] W. Gradl,[39] S. Gramigna,[31a,31b] M. Greco,[82a,82c] M. D. Gu,[56] M. H. Gu,[1,65] C. Y. Guan,[1,71] A. Q. Guo,[34] H. Guo,[55] J. N. Guo,[12,h] L. B. Guo,[46] M. J. Guo,[55] R. P. Guo,[54] X. Guo,[55] Y. P. Guo,[12,h] Z. Guo,[79,65] A. Guskov,[40,b] J. Gutierrez,[29] J. Y. Han,[79,65] T. T. Han,[1] X. Han,[79,65] F. Hanisch,[3] K. D. Hao,[79,65] X. Q. Hao,[20] F. A. Harris,[72] C. Z. He,[51,i] K. K. He,[17,47] K. L. He,[1,71] F. H. Heinsius,[3] C. H. Heinz,[39] Y. K. Heng,[1,65,71] C. Herold,[67] P. C. Hong,[38] G. Y. Hou,[1,71] X. T. Hou,[1,71] Y. R. Hou,[71] Z. L. Hou,[1] H. M. Hu,[1,71] J. F. Hu,[62,k] Q. P. Hu,[79,65] S. L. Hu,[12,h] T. Hu,[1,65,71] Y. Hu,[1] Y. X. Hu,[84] Z. M. Hu,[66] G. S. Huang,[79,65] K. X. Huang,[66] L. Q. Huang,[34,71] P. Huang,[47] X. T. Huang,[55] Y. P. Huang,[1] Y. S. Huang,[66] T. Hussain,[81] N. Hüsken,[39] N. in der Wiesche,[76] J. Jackson,[29] Q. Ji,[1] Q. P. Ji,[20] W. Ji,[1,71] X. B. Ji,[1,71] X. L. Ji,[1,65] Y. Y. Ji,[1] L. K. Jia,[71] X. Q. Jia,[55] D. Jiang,[1,71] H. B. Jiang,[84] S. J. Jiang,[10] X. S. Jiang,[1,65,71] Y. Jiang,[71] J. B. Jiao,[55] J. K. Jiao,[38] Z. Jiao,[25] L. C. L. Jin,[1] S. Jin,[47] Y. Jin,[73] M. Q. Jing,[56] X. M. Jing,[71] T. Johansson,[83] S. Kabana,[36] X. L. Kang,[10] X. S. Kang,[44] B. C. Ke,[89] V. Khachatryan,[29] A. Khoukaz,[76] O. B. Kolcu,[69a] B. Kopf,[3] L. Kröger,[76] L. Krümmel,[3] Y. Y. Kuang,[80] M. Kuessner,[3] X. Kui,[1,71] N. Kumar,[28] A. Kupsc,[49,83] W. Kühn,[41] Q. Lan,[80] W. N. Lan,[20] T. T. Lei,[79,65] M. Lellmann,[39] T. Lenz,[39] C. Li,[52] C. H. Li,[46] C. K. Li,[48] Chunkai Li,[21] Cong Li,[48] D. M. Li,[89] F. Li,[1,65] G. Li,[1] H. B. Li,[1,71] H. J. Li,[20] H. L. Li,[89] H. N. Li,[62,k] H. P. Li,[48] Hui Li,[48] J. N. Li,[32] J. S. Li,[66] J. W. Li,[55] K. Li,[1] K. L. Li,[42,l,m] L. J. Li,[1,71] L. K. Li,[26] Lei Li,[53] M. H. Li,[48] M. R. Li,[1,71] M. T. Li,[55] P. L. Li,[71] P. R. Li,[42,l,m] Q. M. Li,[1,71] Q. X. Li,[55] R. Li,[18,34] S. Li,[89] S. X. Li,[89] S. Y. Li,[89] Shanshan Li,[27,j] T. Li,[55] T. Y. Li,[48] W. D. Li,[1,71] W. G. Li,[1,a] X. Li,[1,71] X. H. Li,[79,65] X. K. Li,[51,i] X. L. Li,[55] X. Y. Li,[1,9] X. Z. Li,[66] Y. Li,[20] Y. B. Li,[85] Y. C. Li,[66] Y. G. Li,[71] Y. P. Li,[38] Z. H. Li,[42] Z. J. Li,[66] Z. L. Li,[89] Z. X. Li,[48] Z. Y. Li,[87] C. Liang,[47] H. Liang,[79,65] Y. F. Liang,[60] Y. T. Liang,[34,71] Z. Z. Liang,[66] G. R. Liao,[14] L. B. Liao,[66] M. H. Liao,[66] Y. P. Liao,[1,71] J. Libby,[28] A. Limphirat,[67] C. C. Lin,[61] C. X. Lin,[34] D. X. Lin,[34,71] T. Lin,[1] B. J. Liu,[1] B. X. Liu,[84] C. Liu,[38] C. X. Liu,[1] F. Liu,[1] F. H. Liu,[59] Feng Liu,[6] G. M. Liu,[62,k] H. Liu,[42,l,m] H. B. Liu,[15] H. M. Liu,[1,71] Huihui Liu,[22] J. B. Liu,[79,65] J. J. Liu,[21] K. Liu,[42,l,m] K. Y. Liu,[44] Ke Liu,[23] Kun Liu,[80] L. Liu,[42] L. C. Liu,[48] Lu Liu,[48] M. H. Liu,[38] P. L. Liu,[55] Q. Liu,[71] S. B. Liu,[79,65] T. Liu,[1] W. M. Liu,[79,65] W. T. Liu,[43] X. Liu,[42,l,m] X. K. Liu,[42,l,m] X. L. Liu,[12,h] X. P. Liu,[12,h] X. T. Liu,[21] X. Y. Liu,[84] Y. Liu,[42,l,m] Y. B. Liu,[48] Yi Liu,[89] Z. A. Liu,[1,65,71] Z. D. Liu,[85] Z. L. Liu,[80] Z. Q. Liu,[55] Z. X. Liu,[1] Z. Y. Liu,[42] X. C. Lou,[1,65,71] H. J. Lu,[25] J. G. Lu,[1,65] X. L. Lu,[16] Y. Lu,[7] Y. H. Lu,[1,71] Y. P. Lu,[1,65] Z. H. Lu,[1,71] C. L. Luo,[46] J. R. Luo,[66] J. S. Luo,[1,71] M. X. Luo,[88] T. Luo,[12,h] X. L. Luo,[1,65] Z. Y. Lv,[23] X. R. Lyu,[71,p] Y. F. Lyu,[48] Y. H. Lyu,[89] F. C. Ma,[44] H. L. Ma,[1] Heng Ma,[27,j] J. L. Ma,[1,71] L. L. Ma,[55] L. R. Ma,[73] Q. M. Ma,[1] R. Q. Ma,[1,71] R. Y. Ma,[20]

T. Ma,[79,65] X. T. Ma,[1,71] X. Y. Ma,[1,65] Y. M. Ma,[34] F. E. Maas,[19] I. MacKay,[77] M. Maggiora,[82a,82c] S. Maity,[34] S. Malde,[77] Q. A. Malik,[81] H. X. Mao,[42,l,m] Y. J. Mao,[51,i] Z. P. Mao,[1] S. Marcello,[82a,82c] A. Marshall,[70] F. M. Melendi,[31a,31b] Y. H. Meng,[71] Z. X. Meng,[73] G. Mezzadri,[31a] H. Miao,[1,71] T. J. Min,[47] R. E. Mitchell,[29] X. H. Mo,[1,65,71] B. Moses,[29] N. Yu. Muchnoi,[4,d] J. Muskalla,[39] Y. Nefedov,[40] F. Nerling,[19,f] H. Neuwirth,[76] Z. Ning,[1,65] S. Nisar,[33] Q. L. Niu,[42,l,m] W. D. Niu,[12,h] Y. Niu,[55] C. Normand,[70] S. L. Olsen,[11,71] Q. Ouyang,[1,65,71] I. V. Ovtin,[4] S. Pacetti,[30b,30c] Y. Pan,[63] A. Pathak,[11] Y. P. Pei,[79,65] M. Pelizaeus,[3] G. L. Peng,[79,65] H. P. Peng,[79,65] X. J. Peng,[42,l,m] Y. Y. Peng,[42,l,m] K. Peters,[13,f] K. Petridis,[70] J. L. Ping,[46] R. G. Ping,[1,71] S. Plura,[39] V. Prasad,[38] L. Pöpping,[3] F. Z. Qi,[1] H. R. Qi,[68] M. Qi,[47] S. Qian,[1,65] W. B. Qian,[71] C. F. Qiao,[71] J. H. Qiao,[20] J. J. Qin,[80] J. L. Qin,[61] L. Q. Qin,[14] L. Y. Qin,[79,65] P. B. Qin,[80] X. P. Qin,[43] X. S. Qin,[55] Z. H. Qin,[1,65] J. F. Qiu,[1] Z. H. Qu,[80] J. Rademacker,[70] K. Ravindran,[74] C. F. Redmer,[39] A. Rivetti,[82c] M. Rolo,[82c] G. Rong,[1,71] S. S. Rong,[1,71] F. Rosini,[30b,30c] Ch. Rosner,[19] M. Q. Ruan,[1,65] N. Salone,[49,r] A. Sarantsev,[40,e] Y. Schelhaas,[39] M. Schernau,[36] K. Schoenning,[83] M. Scodeggio,[31a] W. Shan,[26] X. Y. Shan,[79,65] Z. J. Shang,[42,l,m] J. F. Shangguan,[17] L. G. Shao,[1,71] M. Shao,[79,65] C. P. Shen,[12,h] H. F. Shen,[1,9] W. H. Shen,[71] X. Y. Shen,[1,71] B. A. Shi,[71] Ch. Y. Shi,[87,c] H. Shi,[79,65] J. L. Shi,[8,q] J. Y. Shi,[1] M. H. Shi,[89] S. Y. Shi,[80] X. Shi,[1,65] H. L. Song,[79,65] J. J. Song,[20] M. H. Song,[42] T. Z. Song,[66] W. M. Song,[38] Y. X. Song,[51,i,n] Zirong Song,[27,j] S. Sosio,[82a,82c] S. Spataro,[82a,82c] S. Stansilaus,[77] F. Stieler,[39] M. Stolte,[3] S. S Su,[44] G. B. Sun,[84] G. X. Sun,[1] H. Sun,[71] H. K. Sun,[1] J. F. Sun,[20] K. Sun,[68] L. Sun,[84] R. Sun,[79] S. S. Sun,[1,71] T. Sun,[57,g] W. Y. Sun,[56] Y. C. Sun,[84] Y. H. Sun,[32] Y. J. Sun,[79,65] Y. Z. Sun,[1] Z. Q. Sun,[1,71] Z. T. Sun,[55] H. Tabaharizato,[1] C. J. Tang,[60] G. Y. Tang,[1] J. Tang,[66] J. J. Tang,[79,65] L. F. Tang,[43] Y. A. Tang,[84] Z. H. Tang,[1,71] L. Y. Tao,[80] M. Tat,[77] J. X. Teng,[79,65] J. Y. Tian,[79,65] W. H. Tian,[66] Y. Tian,[34] Z. F. Tian,[84] K. Yu. Todyshev,[4] I. Uman,[69b] E. van der Smagt,[3] B. Wang,[66] Bin Wang,[1] Bo Wang,[79,65] C. Wang,[42,l,m] Chao Wang,[20] Cong Wang,[23] D. Y. Wang,[51,i] F. K. Wang,[66] H. J. Wang,[42,l,m] H. R. Wang,[86] J. Wang,[10] J. J. Wang,[84] J. P. Wang,[37] K. Wang,[1,65] L. L. Wang,[1] L. W. Wang,[38] M. Wang,[55] Mi Wang,[79,65] N. Y. Wang,[71] P. Wang,[21] S. Wang,[42,l,m] Shun Wang,[64] T. Wang,[12,h] W. Wang,[66] W. P. Wang,[39] X. F. Wang,[42,l,m] X. L. Wang,[12,h] X. N. Wang,[1,71] Xin Wang,[27,j] Y. Wang,[1] Y. D. Wang,[50] Y. F. Wang,[1,9,71] Y. H. Wang,[42,l,m] Y. J. Wang,[79,65] Y. L. Wang,[20] Y. N. Wang,[50] Yanning Wang,[84] Yaqian Wang,[18] Yi Wang,[68] Yuan Wang,[18,34] Z. Wang,[1,65] Z. L. Wang,[2] Z. Q. Wang,[12,h] Z. Y. Wang,[1,71] Zhi Wang,[48] Ziyi Wang,[71] D. Wei,[48] D. H. Wei,[14] D. J. Wei,[73] H. R. Wei,[48] F. Weidner,[76] H. R. Wen,[34] S. P. Wen,[1] U. Wiedner,[3] G. Wilkinson,[77] M. Wolke,[83] J. F. Wu,[1,9] L. H. Wu,[1] L. J. Wu,[20] Lianjie Wu,[20] S. G. Wu,[1,71] S. M. Wu,[71] X. W. Wu,[80] Z. Wu,[1,65] H. L. Xia,[79,65] L. Xia,[79,65] B. H. Xiang,[1,71] D. Xiao,[42,l,m] G. Y. Xiao,[47] H. Xiao,[80] Y. L. Xiao,[12,h] Z. J. Xiao,[46] C. Xie,[47] K. J. Xie,[1,71] Y. Xie,[55] Y. G. Xie,[1,65] Y. H. Xie,[6] Z. P. Xie,[79,65] T. Y. Xing,[1,71] D. B. Xiong,[1] G. F. Xu,[1] H. Y. Xu,[2] Q. J. Xu,[17] Q. N. Xu,[32] T. D. Xu,[80] X. P. Xu,[61] Y. Xu,[12,h] Y. C. Xu,[86] Z. S. Xu,[71] F. Yan,[24] L. Yan,[12,h] W. B. Yan,[79,65] W. C. Yan,[89] W. H. Yan,[6] W. P. Yan,[20] X. Q. Yan,[12,h] Y. Y. Yan,[67] H. J. Yang,[57,g] H. L. Yang,[38] H. X. Yang,[1] J. H. Yang,[47] R. J. Yang,[20] X. Y. Yang,[73] Y. Yang,[12,h] Y. G. Yang,[56] Y. H. Yang,[48] Y. M. Yang,[89] Y. Q. Yang,[10] Y. Z. Yang,[20] Youhua Yang,[47] Z. Y. Yang,[80] W. J. Yao,[6] Z. P. Yao,[55] M. Ye,[1,65] M. H. Ye,[9,a] Z. J. Ye,[62,k] K. Yi,[46] Junhao Yin,[48] Z. Y. You,[66] B. X. Yu,[1,65,71] C. X. Yu,[48] G. Yu,[13] J. S. Yu,[27,j] L. W. Yu,[12,h] T. Yu,[80] X. D. Yu,[51,i] Y. C. Yu,[89] Yongchao Yu,[42] C. Z. Yuan,[1,71] H. Yuan,[1,71] J. Yuan,[38] Jie Yuan,[50] L. Yuan,[2] M. K. Yuan,[12,h] S. H. Yuan,[80] Y. Yuan,[1,71] C. X. Yue,[43] Ying Yue,[20] A. A. Zafar,[81] F. R. Zeng,[55] S. H. Zeng,[70] X. Zeng,[12,h] Y. J. Zeng,[1,71] Yujie Zeng,[66] Y. C. Zhai,[55] Y. H. Zhan,[66] B. L. Zhang,[1,71] B. X. Zhang,[1,a] D. H. Zhang,[48] G. Y. Zhang,[20] Gengyuan Zhang,[1,71] H. Zhang,[79,65] H. C. Zhang,[1,65,71] H. H. Zhang,[66] H. Q. Zhang,[1,65,71] H. R. Zhang,[79,65] H. Y. Zhang,[1,65] Han Zhang,[89] J. Zhang,[66] J. J. Zhang,[58] J. L. Zhang,[21] J. Q. Zhang,[46] J. S. Zhang,[12,h] J. W. Zhang,[1,65,71] J. X. Zhang,[42,l,m] J. Y. Zhang,[1] J. Z. Zhang,[1,71] Jianyu Zhang,[71] Jin Zhang,[53] Jiyuan Zhang,[12,h] L. M. Zhang,[68] Lei Zhang,[47] N. Zhang,[38] P. Zhang,[1,9] Q. Zhang,[20] Q. Y. Zhang,[38] Q. Z. Zhang,[71] R. Y. Zhang,[42,l,m] S. H. Zhang,[1,71] S. N. Zhang,[77] Shulei Zhang,[27,j] X. M. Zhang,[1] X. Y. Zhang,[55] Y. T. Zhang,[89] Y. H. Zhang,[1,65] Y. P. Zhang,[79,65] Yao Zhang,[1] Yu Zhang,[80] Yu Zhang,[66] Z. Zhang,[34] Z. D. Zhang,[1] Z. H. Zhang,[1] Z. L. Zhang,[38] Z. X. Zhang,[20] Z. Y. Zhang,[84] Zh. Zh. Zhang,[20] Zhilong Zhang,[61] Ziyang Zhang,[50] Ziyu Zhang,[48] G. Zhao,[1] J.-P. Zhao,[71] J. Y. Zhao,[1,71] J. Z. Zhao,[1,65] L. Zhao,[1] Lei Zhao,[79,65] M. G. Zhao,[48] R. P. Zhao,[71] S. J. Zhao,[89] Y. B. Zhao,[1,65] Y. L. Zhao,[61] Y. P. Zhao,[50] Y. X. Zhao,[34,71] Z. G. Zhao,[79,65] A. Zhemchugov,[40,b] B. Zheng,[80] B. M. Zheng,[38] J. P. Zheng,[1,65]

W. J. Zheng,[1,71] W. Q. Zheng,[10] X. R. Zheng,[20] Y. H. Zheng,[71,p] B. Zhong,[46] C. Zhong,[20] X. Zhong,[45] H. Zhou,[39,55,o] J. Q. Zhou,[38] S. Zhou,[6] X. Zhou,[84] X. K. Zhou,[6] X. R. Zhou,[79,65] X. Y. Zhou,[43] Y. X. Zhou,[86] Y. Z. Zhou,[20] A. N. Zhu,[71] J. Zhu,[48] K. Zhu,[1] K. J. Zhu,[1,65,71] K. S. Zhu,[12,h] L. X. Zhu,[71] Lin Zhu,[20] S. H. Zhu,[78] T. J. Zhu,[12,h] W. D. Zhu,[12,h] W. J. Zhu,[1] W. Z. Zhu,[20] Y. C. Zhu,[79,65] Z. A. Zhu,[1,71] X. Y. Zhuang,[48] M. Zhuge,[55] J. H. Zou,[1] and J. Zu[34]

(BESIII Collaboration)

[1]*Institute of High Energy Physics, Beijing 100049, People's Republic of China*
[2]*Beihang University, Beijing 100191, People's Republic of China*
[3]*Bochum Ruhr-University, D-44780 Bochum, Germany*
[4]*Budker Institute of Nuclear Physics SB RAS (BINP), Novosibirsk 630090, Russia*
[5]*Carnegie Mellon University, Pittsburgh, Pennsylvania 15213, USA*
[6]*Central China Normal University, Wuhan 430079, People's Republic of China*
[7]*Central South University, Changsha 410083, People's Republic of China*
[8]*Chengdu University of Technology, Chengdu 610059, People's Republic of China*
[9]*China Center of Advanced Science and Technology, Beijing 100190, People's Republic of China*
[10]*China University of Geosciences, Wuhan 430074, People's Republic of China*
[11]*Chung-Ang University, Seoul, 06974, Republic of Korea*
[12]*Fudan University, Shanghai 200433, People's Republic of China*
[13]*GSI Helmholtzcentre for Heavy Ion Research GmbH, D-64291 Darmstadt, Germany*
[14]*Guangxi Normal University, Guilin 541004, People's Republic of China*
[15]*Guangxi University, Nanning 530004, People's Republic of China*
[16]*Guangxi University of Science and Technology, Liuzhou 545006, People's Republic of China*
[17]*Hangzhou Normal University, Hangzhou 310036, People's Republic of China*
[18]*Hebei University, Baoding 071002, People's Republic of China*
[19]*Helmholtz Institute Mainz, Staudinger Weg 18, D-55099 Mainz, Germany*
[20]*Henan Normal University, Xinxiang 453007, People's Republic of China*
[21]*Henan University, Kaifeng 475004, People's Republic of China*
[22]*Henan University of Science and Technology, Luoyang 471003, People's Republic of China*
[23]*Henan University of Technology, Zhengzhou 450001, People's Republic of China*
[24]*Hengyang Normal University, Hengyang 421001, People's Republic of China*
[25]*Huangshan College, Huangshan 245000, People's Republic of China*
[26]*Hunan Normal University, Changsha 410081, People's Republic of China*
[27]*Hunan University, Changsha 410082, People's Republic of China*
[28]*Indian Institute of Technology Madras, Chennai 600036, India*
[29]*Indiana University, Bloomington, Indiana 47405, USA*
[30a]*INFN Laboratori Nazionali di Frascati, I-00044, Frascati, Italy*
[30b]*INFN Sezione di Perugia, I-06100, Perugia, Italy*
[30c]*University of Perugia, I-06100, Perugia, Italy*
[31a]*INFN Sezione di Ferrara, I-44122, Ferrara, Italy*
[31b]*University of Ferrara, I-44122, Ferrara, Italy*
[32]*Inner Mongolia University, Hohhot 010021, People's Republic of China*
[33]*Institute of Business Administration, University Road, Karachi, 75270 Pakistan*
[34]*Institute of Modern Physics, Lanzhou 730000, People's Republic of China*
[35]*Institute of Physics and Technology, Mongolian Academy of Sciences, Peace Avenue 54B, Ulaanbaatar 13330, Mongolia*
[36]*Instituto de Alta Investigación, Universidad de Tarapacá, Casilla 7D, Arica 1000000, Chile*
[37]*Jiangsu Ocean University, Lianyungang 222000, People's Republic of China*
[38]*Jilin University, Changchun 130012, People's Republic of China*
[39]*Johannes Gutenberg University of Mainz, Johann-Joachim-Becher-Weg 45, D-55099 Mainz, Germany*
[40]*Joint Institute for Nuclear Research, 141980 Dubna, Moscow region, Russia*
[41]*Justus-Liebig-Universitaet Giessen, II. Physikalisches Institut, Heinrich-Buff-Ring 16, D-35392 Giessen, Germany*
[42]*Lanzhou University, Lanzhou 730000, People's Republic of China*
[43]*Liaoning Normal University, Dalian 116029, People's Republic of China*
[44]*Liaoning University, Shenyang 110036, People's Republic of China*
[45]*Longyan University, Longyan 364000, People's Republic of China*

[46]*Nanjing Normal University, Nanjing 210023, People's Republic of China*
[47]*Nanjing University, Nanjing 210093, People's Republic of China*
[48]*Nankai University, Tianjin 300071, People's Republic of China*
[49]*National Centre for Nuclear Research, Warsaw 02-093, Poland*
[50]*North China Electric Power University, Beijing 102206, People's Republic of China*
[51]*Peking University, Beijing 100871, People's Republic of China*
[52]*Qufu Normal University, Qufu 273165, People's Republic of China*
[53]*Renmin University of China, Beijing 100872, People's Republic of China*
[54]*Shandong Normal University, Jinan 250014, People's Republic of China*
[55]*Shandong University, Jinan 250100, People's Republic of China*
[56]*Shandong University of Technology, Zibo 255000, People's Republic of China*
[57]*Shanghai Jiao Tong University, Shanghai 200240, People's Republic of China*
[58]*Shanxi Normal University, Linfen 041004, People's Republic of China*
[59]*Shanxi University, Taiyuan 030006, People's Republic of China*
[60]*Sichuan University, Chengdu 610064, People's Republic of China*
[61]*Soochow University, Suzhou 215006, People's Republic of China*
[62]*South China Normal University, Guangzhou 510006, People's Republic of China*
[63]*Southeast University, Nanjing 211100, People's Republic of China*
[64]*Southwest University of Science and Technology, Mianyang 621010, People's Republic of China*
[65]*State Key Laboratory of Particle Detection and Electronics, Beijing 100049, Hefei 230026, People's Republic of China*
[66]*Sun Yat-Sen University, Guangzhou 510275, People's Republic of China*
[67]*Suranaree University of Technology, University Avenue 111, Nakhon Ratchasima 30000, Thailand*
[68]*Tsinghua University, Beijing 100084, People's Republic of China*
[69a]*Turkish Accelerator Center Particle Factory Group, Istinye University, 34010, Istanbul, Turkey*
[69b]*Near East University, Nicosia, North Cyprus, 99138, Mersin 10, Turkey*
[70]*University of Bristol, H H Wills Physics Laboratory, Tyndall Avenue, Bristol, BS8 1TL, United Kingdom*
[71]*University of Chinese Academy of Sciences, Beijing 100049, People's Republic of China*
[72]*University of Hawaii, Honolulu, Hawaii 96822, USA*
[73]*University of Jinan, Jinan 250022, People's Republic of China*
[74]*University of La Serena, Av. Raúl Bitrán 1305, La Serena, Chile*
[75]*University of Manchester, Oxford Road, Manchester, M13 9PL, United Kingdom*
[76]*University of Muenster, Wilhelm-Klemm-Strasse 9, 48149 Muenster, Germany*
[77]*University of Oxford, Keble Road, Oxford OX13RH, United Kingdom*
[78]*University of Science and Technology Liaoning, Anshan 114051, People's Republic of China*
[79]*University of Science and Technology of China, Hefei 230026, People's Republic of China*
[80]*University of South China, Hengyang 421001, People's Republic of China*
[81]*University of the Punjab, Lahore-54590, Pakistan*
[82a]*University of Turin and INFN, University of Turin, I-10125, Turin, Italy*
[82b]*University of Eastern Piedmont, I-15121, Alessandria, Italy*
[82c]*INFN, I-10125, Turin, Italy*
[83]*Uppsala University, Box 516, SE-75120 Uppsala, Sweden*
[84]*Wuhan University, Wuhan 430072, People's Republic of China*
[85]*Xi'an Jiaotong University, No.28 Xianning West Road, Xi'an, Shaanxi 710049, People's Republic of China*
[86]*Yantai University, Yantai 264005, People's Republic of China*
[87]*Yunnan University, Kunming 650500, People's Republic of China*
[88]*Zhejiang University, Hangzhou 310027, People's Republic of China*
[89]*Zhengzhou University, Zhengzhou 450001, People's Republic of China*

[a]Deceased.
[b]Also at the Moscow Institute of Physics and Technology, Moscow 141700, Russia.
[c]Also at the Functional Electronics Laboratory, Tomsk State University, Tomsk, 634050, Russia.
[d]Also at the Novosibirsk State University, Novosibirsk, 630090, Russia.
[e]Also at the NRC "Kurchatov Institute", PNPI, 188300, Gatchina, Russia.
[f]Also at Goethe University Frankfurt, 60323 Frankfurt am Main, Germany.
[g]Also at Key Laboratory for Particle Physics, Astrophysics and Cosmology, Ministry of Education; Shanghai Key Laboratory for Particle Physics and Cosmology; Institute of Nuclear and Particle Physics, Shanghai 200240, People's Republic of China.
[h]Also at Key Laboratory of Nuclear Physics and Ion-beam Application (MOE) and Institute of Modern Physics, Fudan University, Shanghai 200443, People's Republic of China.

[i]Also at State Key Laboratory of Nuclear Physics and Technology, Peking University, Beijing 100871, People's Republic of China.
[j]Also at School of Physics and Electronics, Hunan University, Changsha 410082, China.
[k]Also at Guangdong Provincial Key Laboratory of Nuclear Science, Institute of Quantum Matter, South China Normal University, Guangzhou 510006, China.
[l]Also at MOE Frontiers Science Center for Rare Isotopes, Lanzhou University, Lanzhou 730000, People's Republic of China.
[m]Also at Lanzhou Center for Theoretical Physics, Lanzhou University, Lanzhou 730000, People's Republic of China.
[n]Also at Ecole Polytechnique Federale de Lausanne (EPFL), CH-1015 Lausanne, Switzerland.
[o]Also at Helmholtz Institute Mainz, Staudinger Weg 18, D-55099 Mainz, Germany.
[p]Also at Hangzhou Institute for Advanced Study, University of Chinese Academy of Sciences, Hangzhou 310024, China.
[q]Also at Applied Nuclear Technology in Geosciences Key Laboratory of Sichuan Province, Chengdu University of Technology, Chengdu 610059, People's Republic of China.
[r]Currently at University of Silesia in Katowice, Institute of Physics, 75 Pulku Piechoty 1, 41-500 Chorzow, Poland.